

# Lithographically Defined Plasmonic Graphene Antennas for Terahertz-Band Communication

Luke Zakrajsek, Erik Einarsson, *Member, IEEE*, Ngwe Thawdar, *Member, IEEE*, Michael Medley, *Senior Member, IEEE*, and Josep Miquel Jornet, *Member, IEEE*

(Invited Paper)

**Abstract**—Graphene-based plasmonic antennas could enable ultrabroadband communication among nanodevices in the Terahertz band (0.1–10 THz). Despite significant progress in graphene synthesis, the fabrication, manipulation, and placement of precisely formed graphene-based nanostructures still pose many practical challenges. In this letter, by comparing analytical solutions with numerical simulations, we show that lithographically defined graphene antennas, circumscribed by a focused ion beam (FIB), should behave as though they were electromagnetically isolated provided the width of the surrounding cut is comparable to the plasmonic wavelength. This result opens the door to practical and more advanced antenna designs.

**Index Terms**—Graphene plasmonics, nano-antennas, nanonetworks, terahertz band.

## I. INTRODUCTION

NANOTECHNOLOGY is providing the engineering community with a new set of tools to design and manufacture novel nanoscale devices able to perform specific tasks such as computing, data storing, sensing, and actuation. The integration of several of these nanodevices into a single entity will enable the development of advanced nanoscale machines. By means of communication, nanomachines will be able to coordinate with each other and perform more complex tasks in a distributed fashion. The resulting nanonetworks will enable many new applications—such as nanosensor networks for chemical and biological agents or massive multicore on-chip processing architectures—in the consumer, industrial, biomedical, and military fields [1].

One of the most promising means to enable communication between nanomachines relies on the use of graphene-based nano-antennas. Graphene is a two-dimensional carbon crystal with numerous outstanding physical properties, such as excellent electrical conductivity, which makes it very well suited for propagating extremely high-frequency electrical signals [2], [3]. Moreover, graphene supports the propagation of surface plas-

mon polariton (SPP) waves at Terahertz (THz)-band frequencies (0.1–10 THz) [4], [5]. SPP waves are confined electromagnetic (EM) waves coupled to electric charges at the interface between a metal (e.g., graphene) and a dielectric.

By leveraging the propagation properties of SPP waves on graphene, novel nano-antennas suited for the expected size of nanomachines can be developed. In particular, as first shown in [6] by using the transmission line formalism, a graphene-based antenna just 1  $\mu\text{m}$  long and several hundreds of nanometers wide can be designed to resonate in the THz band. This frequency is two orders of magnitude lower than the resonance frequency of a metallic antenna with comparable dimensions. To date, there are many studies on the properties and potential applications of graphene-based antennas, including electrically tunable [7], reconfigurable [8], and beamforming antennas [9]. However, despite progress in graphene synthesis, the fabrication, manipulation, and placement of precisely formed graphene-based nanostructures with well-defined geometry pose many practical challenges.

To address these limitations, we propose to directly cut nano-antennas out of a larger graphene sheet. More specifically, instead of defining a resonant cavity and removing all excess graphene, we propose to create a resonant cavity with well-defined boundaries *within* a larger graphene layer.

## II. TOP-DOWN NANO-ANTENNA FABRICATION METHODS

For an application in which electrical conductivity is paramount, graphene with large grain size is desired. This can be obtained by various methods, but chemical vapor deposition (CVD) is arguably the most economical and widely used. In this method, graphene is grown on the surface of a copper foil at high temperature (900°–1000 °C). Carbon is provided in vapor form (usually as CH<sub>4</sub>), and graphene forms on the Cu foil via a surface-mediated reaction. With appropriate surface treatments and synthesis conditions, single-crystal graphene grains millimeters in size can be reliably produced [10], [11]. While this method produces sufficiently large single crystals, the as-synthesized graphene must be transferred onto a target substrate, which is usually a Si wafer covered by a SiO<sub>2</sub> oxide layer. With the graphene in place on the target substrate, the next step is to form the antenna into the desired shape. The two general approaches to doing this are: 1) remove everything except the desired area (etching), and 2) isolate the desired area by cutting (see Fig. 1).

Etching can be achieved by either wet (chemical) or dry (plasma) methods. Meanwhile, rather simple wet etching comes with significant drawbacks. Most importantly, the graphene

Manuscript received October 2, 2015; accepted January 27, 2016. Date of publication February 8, 2016; date of current version June 2, 2016. This work was supported by the AFRL under AFRL Grant FA8750-15-1-0050.

L. Zakrajsek, E. Einarsson, and J. M. Jornet are with the Department of Electrical Engineering, University at Buffalo, The State University of New York, Buffalo, NY 14260 USA (e-mail: lukezagr@buffalo.edu; erikeina@buffalo.edu; jmjornet@buffalo.edu).

N. Thawdar and M. Medley are with the Air Force Research Laboratory/RI, Rome, NY 13441 USA (e-mail: ngwe.thawdar@us.af.mil; michael.medley@us.af.mil).

Color versions of one or more of the figures in this letter are available online at <http://ieeexplore.ieee.org>.

Digital Object Identifier 10.1109/LAWP.2016.2527001

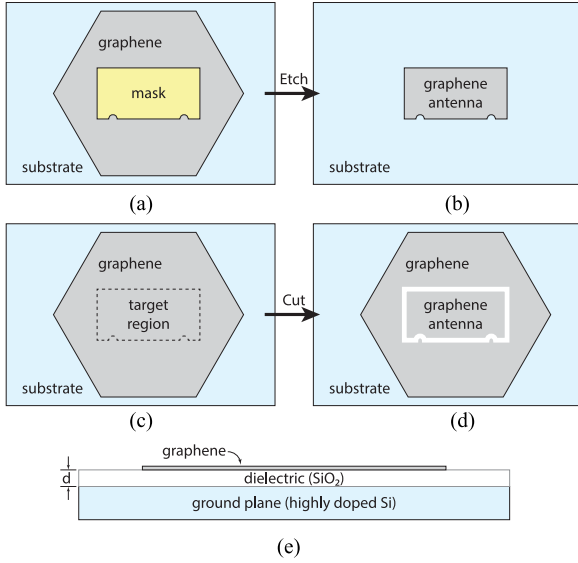


Fig. 1. (a) Graphene on substrate with target antenna region masked, (b) remaining graphene patch after etching and mask removal, (c) graphene on substrate with target antenna region identified, (d) graphene after circumscribing target region with ion beam, and (e) cross section of system showing graphene, dielectric, and ground plane.

region to be retained must be covered and protected during the etching process. This introduces an additional processing step, during which the graphene could be damaged or degraded. Furthermore, extremely precise etching is difficult to control, and well-defined edges and complicated structures are very difficult to obtain.

Much better control can be achieved using a direct lithographic method, in which a focused ion beam (FIB) is used to remove or destroy a narrow region around a desired shape. We will refer to this approach as “outlining.” It has been shown that a cut width of 15 nm is sufficient to electrically isolate a graphene region [12], and we show in Section IV that a region can be *electromagnetically* isolated with a moderately wider cut. Here, we propose a way to combine these widely used methods (CVD and FIB) to fabricate THz-band graphene antennas.

### III. ANALYTICAL MODEL OF LITHOGRAPHICALLY DEFINED NANO-ANTENNAS

Analysis of the outlined nano-antennas requires characterization of the SPP propagation properties on graphene. These properties depend on the conductivity of the graphene sheet. In this section, we first recall the conductivity model that will be utilized in our analysis. We then obtain the plasmonic wavelength and the antenna resonant length.

#### A. Complex Conductivity Model of Graphene

In the following analysis, we consider a surface conductivity model for infinitely large graphene sheets obtained using the Kubo formalism [13], [14]. This is given by

$$\sigma^g = \sigma_{\text{intra}}^g + \sigma_{\text{inter}}^g \quad (1)$$

$$\sigma_{\text{intra}}^g = i \frac{2e^2}{\pi \hbar^2} \frac{k_B T}{\omega + i\tau_g^{-1}} \ln \left( 2 \cosh \left( \frac{E_F}{2k_B T} \right) \right) \quad (2)$$

$$\sigma_{\text{inter}}^g = \frac{e^2}{4\hbar} \left( H \left( \frac{\omega}{2} \right) + i \frac{4\omega}{\pi} \int_0^\infty \frac{H(\epsilon) - H(\omega/2)}{\omega^2 - 4\epsilon^2} d\epsilon \right) \quad (3)$$

and

$$H(a) = \frac{\sinh(\hbar a/k_B T)}{\cosh(E_F/k_B T) + \cosh(\hbar a/k_B T)} \quad (4)$$

where  $\omega = 2\pi f$ ,  $\hbar = h/2\pi$  is the reduced Planck's constant,  $e$  is the electron charge,  $k_B$  is the Boltzmann constant,  $T$  is temperature,  $\tau_g$  is the relaxation time of electrons in graphene, and  $E_F$  refers to the Fermi energy of the graphene sheet. This can be easily modified by means of electrostatic bias or gating of the graphene layer, enabling the aforementioned tuning of the nano-antenna frequency response.

As we showed in [15], a more accurate conductivity model can be developed by taking into account the impact of lateral electron confinement in graphene nanoribbons, but the two models converge for graphene strips which are 50 nm wide or more. In our analysis, we consider only plasmonic resonant cavities which are several hundred nanometers wide. Finally, from [13] and [14], it is important to note that the conductivity model described by (1) and the following was derived by neglecting the spatial dispersion of the ac field. Therefore, it can be used for analysis of the SPP propagation only in the long wavelength limit, i.e.,  $k_{\text{spp}} \ll \omega/v_F$ , where  $k_{\text{spp}}$  is the SPP wavenumber and  $v_F \approx 8 \times 10^5 \text{ ms}^{-1}$  is the Fermi velocity of Dirac fermions in graphene.

#### B. Dispersion Equation for SPP Waves

The propagation properties of SPP waves can be obtained by deriving and solving the SPP wave dispersion equation on graphene. In the aforementioned nano-antenna-related works [7]–[9], the dispersion equation was obtained by considering a graphene layer at the interface between two infinitely large dielectric materials, usually between air and silicon dioxide ( $\text{SiO}_2$ ). However, as we discussed in Section II, our antenna relies on the presence of a metallic ground plane at a distance  $d$  from the graphene layer. This is needed both to create the resonant patch as well as to control the Fermi energy of the graphene layer and tune its conductivity.

From [16], the dispersion equation for transverse magnetic (TM) SPP waves in gated graphene structures in the quasi-static regime—i.e., for  $k_{\text{spp}} \gg \omega/c$ , where  $c$  is the speed of light—is given by

$$-i \frac{\sigma^g}{\omega \epsilon_0} = \frac{\epsilon_1 + \epsilon_2 \coth(k_{\text{spp}} d)}{k_{\text{spp}}} \quad (5)$$

where  $\sigma^g$  is the conductivity of graphene given by (1),  $\epsilon_1$  is the relative permittivity of the dielectric above the graphene layer, and  $\epsilon_2$  is the relative permittivity of the dielectric between the graphene layer and the metallic ground plane, which are separated by a distance  $d$ . It can be easily shown by taking the limit as  $d \rightarrow \infty$  that (5) tends to the quasi-static dispersion equation of SPP waves in ungated graphene used in the aforementioned works. Unfortunately, a closed-form expression for  $k_{\text{spp}}$  in the general case does not exist, but can only be obtained numerically.

### C. Plasmonic Antenna Frequency Response

Contrary to previous findings, the proposed nano-antenna is not composed of an isolated graphene strip, but has been defined within a larger graphene flake. Intuitively, an antenna that has been circumscribed within a larger graphene flake should behave as an isolated antenna, provided that the cut thickness is sufficiently large that it acts as a strict boundary for the propagation of SPP waves. This will be the case if the cut thickness  $t$  is large in terms of the SPP wavelength  $\lambda_{\text{spp}}$ . This last term can be determined from the real part of the SPP wave vector by

$$\lambda_{\text{spp}} = \frac{2\pi}{\text{Re}\{k_{\text{spp}}\}}. \quad (6)$$

Under this condition, the lithographically defined nano-antenna is expected to behave as an isolated nano-antenna. For example, the TM fundamental resonant frequency or, equivalently, the antenna resonant length is obtained by

$$L = \frac{\lambda_{\text{spp}}}{2} = \frac{\pi}{\text{Re}\{k_{\text{spp}}\}}. \quad (7)$$

Other relevant magnitudes, including the antenna input impedance, currents, and fields distribution on the outlined cavity can be similarly characterized.

## IV. SIMULATION AND NUMERICAL RESULTS

Here, we validate our models and analyze the performance of the proposed outlined nano-antennas by means of EM simulations with COMSOL Multiphysics. Graphene is modeled as a transition boundary condition with complex dynamic conductivity given by (1), where  $\tau_g = 0.5$  ps and  $E_F = 1.25$  eV at  $T = 300$  K. These values are based on analysis of Raman spectra obtained from CVD-grown graphene. The graphene layer rests on top of a 90-nm-thick  $\text{SiO}_2$  dielectric ( $\epsilon_r = 4$ ), which separates the graphene from the ground plane. This thickness is chosen because it maximizes visual detection of graphene on  $\text{SiO}_2$  [17]. Unless otherwise stated, the graphene antenna is outlined with a cut width equal to 500 nm. The antenna is fed with a lumped port that connects the graphene layer to the ground plane on one side. In a practical setup, the feeding of the antenna could be realized by means of a plasma wave source based on a high-electron-mobility transistor and built with a III-V semiconductor material, such as those proposed in [18] and [19]. A perfectly matched layer and a scattering boundary condition are utilized to minimize the impact of simulating a finite space. The antenna is meshed with a resolution of  $\lambda_{\text{spp}}/5$ .

### A. Validation of the SPP Dispersion Model

In Fig. 2, we illustrate and compare the antenna resonant length as a function of frequency for the following three cases: 1) when using the SPP wave dispersion equation for gated graphene given by (5); 2) obtained by simulation with COMSOL Multiphysics; and 3) when using the dispersion equation for ungated graphene from the aforementioned works. The results show that the revised SPP wave dispersion equation for gated graphene is able to accurately reproduce the simulation results. The impact of the ground plane is not negligible, as it effectively changes the resonant length by one order of magnitude by increasing the SPP wave confinement factor.

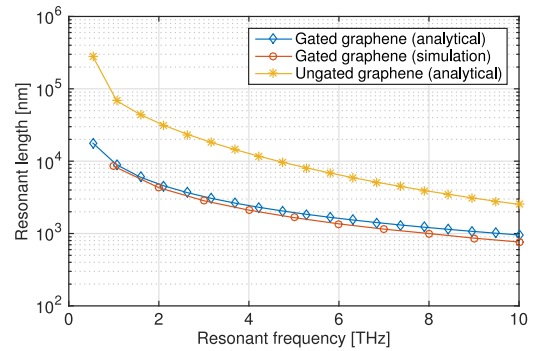


Fig. 2. Antenna resonant length as a function of frequency according to the SPP dispersion models for gated and ungated graphene, and obtained by simulation.

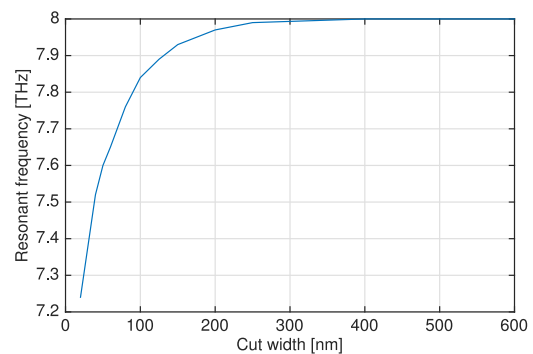


Fig. 3. Antenna resonant frequency as a function of cut width.

### B. Impact of the Cut Width

We now fix the size of the graphene-based nano-antenna to be  $1000 \times 1000$  nm<sup>2</sup> and analyze the impact of the cut width. The antenna resonant frequency is 8 THz. At this frequency, both the long-wavelength condition and the quasi-static condition are simultaneously met ( $v_F \ll v_{\text{spp}} \ll c$ ). In Fig. 3, we illustrate the antenna resonant frequency as a function of the cut width, ranging from 25 to 600 nm, which corresponds to  $t \ll \lambda_{\text{spp}}/2$  and  $t > \lambda_{\text{spp}}/2$ , respectively, at the resonant frequency. This result clearly shows that the antenna is effectively isolated provided that the cut width is at least comparable to  $\lambda_{\text{spp}}/2$ . This also means that there is no significant coupling due to the radiated waves in free space.

In addition, to explain the behavior of the resonant frequency, we illustrate in Fig. 4 the  $z$ -component of the electric field on the nano-antenna when considering a completely etched antenna as well as cut antennas with cut widths of 25 and 500 nm. As intuitively described in Section III, the etched antenna and the cut antenna behave almost identically, provided that the cut is not only wide enough to electrically break the structure but also to minimize the coupling between the active patch and the remaining graphene sheet. For narrower cut widths, the coupling between the antenna and the graphene flakes affects the antenna input impedance and, thus, the antenna resonant frequency. This can also be seen in Fig. 5, where the antenna input impedance is shown as a function of the cut width. As the cut width increases, the real part of the impedance increases

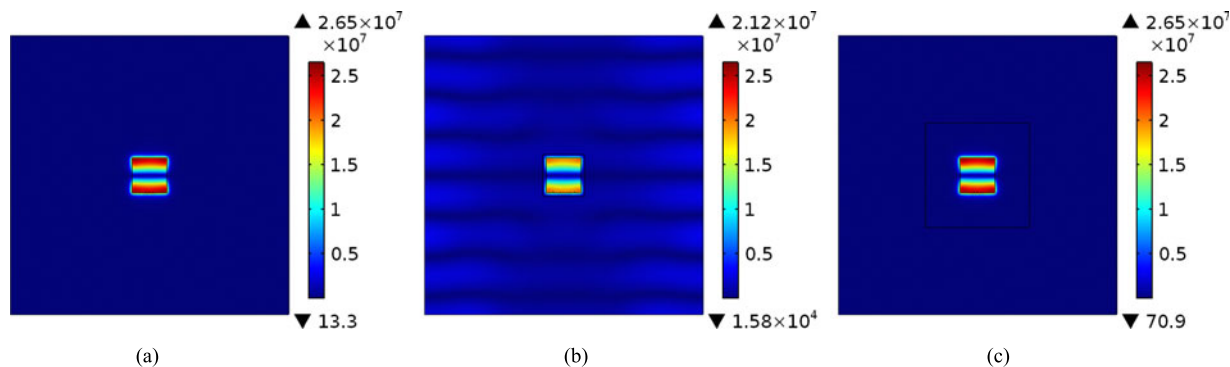


Fig. 4. Electric field of a nano-antenna that has been (a) etched, (b) cut with  $t = 50$  nm, and (c) cut with  $t = 500$  nm.

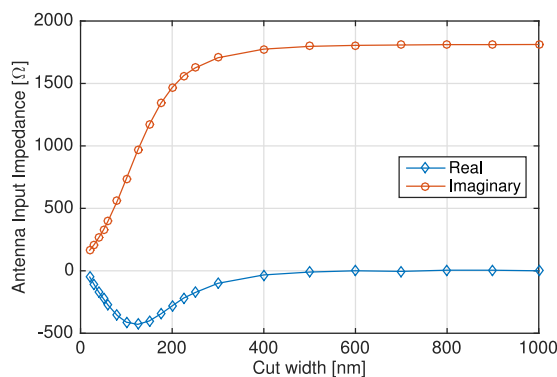


Fig. 5. Antenna input impedance as a function of the cut width.

until reaching that of the isolated antenna [20], almost 1.8 k $\Omega$ . This is consistent with the fact that smaller graphene flakes have a higher contact resistance than infinitely large patches. The imaginary part of the impedance first is negative and then quickly tends to 0  $\Omega$ , which is needed for the cavity to resonate.

## V. CONCLUSION

We have proposed to lithographically define plasmonic nano-antennas on graphene by means of an ion beam. Our analytical and numerical results show that outlined nano-antennas effectively behave as their isolated counterparts, provided that the cut width is comparable to the plasmonic wavelength. The possibility to define antennas in this way on larger graphene flakes opens the door to innovative antenna designs, such as fractal or log-periodic graphene-based nano-antennas, which could not be obtained by means of conventional etching. Moreover, this suggests the possibility of defining multiple antennas, i.e., an antenna array, within a larger graphene sheet.

## ACKNOWLEDGMENT

The State University of New York at Buffalo would like to thank the U.S. Government's support in the publication of this letter. Any opinions, findings and conclusions or recommendations expressed in this material are those of the author(s) and do not necessarily reflect the views of the AFRL.

## REFERENCES

- [1] I. F. Akyildiz and J. M. Jornet, "The internet of nano-things," *IEEE Wireless Commun.*, vol. 17, no. 6, pp. 58–63, Dec. 2010.
- [2] K. S. Novoselov *et al.*, "A roadmap for graphene," *Nature*, vol. 490, no. 7419, pp. 192–200, 2012.
- [3] A. C. Ferrari *et al.*, "Science and technology roadmap for graphene, related two-dimensional crystals, and hybrid systems," *Nanoscale*, vol. 7, no. 11, pp. 4598–4810, 2015.
- [4] L. Ju *et al.*, "Graphene plasmonics for tunable terahertz metamaterials," *Nature Nanotechnol.*, vol. 6, pp. 630–634, Sep. 2011.
- [5] F. H. L. Koppens, D. E. Chang, and F. J. Garcia de Abajo, "Graphene plasmonics: A platform for strong light matter interactions," *Nano Lett.*, vol. 11, no. 8, pp. 3370–3377, Aug. 2011.
- [6] J. M. Jornet and I. F. Akyildiz, "Graphene-based nano-antennas for electromagnetic nanocommunications in the terahertz band," in *Proc. 4th Eur. Conf. Antennas Propag.*, Apr. 2010, pp. 1–5.
- [7] I. Llatser *et al.*, "Graphene-based nano-patch antenna for terahertz radiation," *Photon. Nanostruct., Fundam. Appl.*, vol. 10, no. 4, pp. 353–358, Oct. 2012.
- [8] M. Tamagnone, J. S. Gomez-Diaz, J. R. Mosig, and J. Perruisseau-Carrier, "Reconfigurable terahertz plasmonic antenna concept using a graphene stack," *Appl. Phys. Lett.*, vol. 101, no. 21, p. 214102, 2012.
- [9] M. Aldrigo, M. Dragoman, and D. Dragoman, "Smart antennas based on graphene," *J. Appl. Phys.*, vol. 116, no. 11, p. 114302, 2014.
- [10] Y. Hao *et al.*, "The role of surface oxygen in the growth of large single-crystal graphene on copper," *Science*, vol. 342, no. 6159, pp. 720–723, 2013.
- [11] X. Chen *et al.*, "Chemical vapor deposition growth of 5 mm hexagonal single-crystal graphene from ethanol," *Carbon*, vol. 94, pp. 810–815, 2015.
- [12] V. Iberi *et al.*, "Maskless lithography and in situ visualization of conductivity of graphene using helium ion microscopy," *Sci. Rep.*, vol. 5, p. 11952, 2015.
- [13] L. Falkovsky and A. A. Varlamov, "Space-time dispersion of graphene conductivity," *Eur. Phys. J. B*, vol. 56, pp. 281–284, 2007.
- [14] G. W. Hanson, "Dyadic Green's functions and guided surface waves for a surface conductivity model of graphene," *J. Appl. Phys.*, vol. 103, no. 6, p. 064302, 2008.
- [15] J. M. Jornet and I. F. Akyildiz, "Graphene-based plasmonic nano-antenna for terahertz band communication in nanonetworks," *IEEE J. Sel. Areas Commun.*, vol. 31, no. 12, pp. 685–694, Dec. 2013.
- [16] V. Ryzhii, "Terahertz plasma waves in gated graphene heterostructures," *Jpn. J. Appl. Phys.*, vol. 45, no. 9L, pp. L923–L925, 2006.
- [17] P. Blake *et al.*, "Making graphene visible," *Appl. Phys. Lett.*, vol. 91, no. 6, p. 063124, 2007.
- [18] W. Knap, F. Teppe, N. Dyakonova, D. Coquillat, and J. Lusakowski, "Plasma wave oscillations in nanometer field effect transistors for terahertz detection and emission," *J. Phys., Condens. Matter*, vol. 20, no. 38, p. 384205, 2008.
- [19] J. M. Jornet and I. F. Akyildiz, "Graphene-based plasmonic nano-transceiver for terahertz band communication," in *Proc. 8th Eur. Conf. Antennas Propag.*, Apr. 2014, pp. 492–496.
- [20] M. Tamagnone and J. Perruisseau-Carrier, "Predicting input impedance and efficiency of graphene reconfigurable dipoles using a simple circuit model," *IEEE Antennas Wireless Propag. Lett.*, vol. 13, pp. 313–316, 2014.